Enhancing sustainability and performance in alkali-activated mortars with recycled rubber aggregates subjected to varied curing methods

Abdelhafid Benammar[a], Ammar Noui[b], Abdelatif Benouadah[c],Nabil Maafi[d], Oussama Kessal[e], Meriem Dridi[f], Ahmed Abderraouf Belkadi[g]

Department of Civil Engineering, Faculty of Sciences and Technology, University Mohamed El Bachir El Ibrahimi of Bordj Bou Arreridj, ElAnasser, 34030, Algeria

Article Info	Abstract
	Rubber waste represents a significant waste stream that can be used as a substitute for natural aggregates in concrete. The main objective of this innovative study is to evaluate the effectiveness of alkali-activated mortars (AAM) incorporating recycled rubber aggregates in the development of an environmentally friendly construction material. Different replacement rates of sand with rubber particles (10%, 20%, and 30% by volume) are analysed. Rubberized alkali-activated mortars (RAAM) were produced using a combination of 10 M sodium hydroxide (NaOH) and a $Na_2SiO_3/NaOH$ ratio of 3. Additionally, the influence of three curing methods on the properties of RAAM is also examined: air drying, curing in a climate chamber, or in an oven. The properties of RAAM were evaluated through tests including the flow table test, density test, water absorption test, and compressive strength test. Furthermore, the study also assessed the cost-effectiveness and environmental impact of RAAM. This variable study is complemented by an ANOVA parametric analysis. The results show a decrease in the compressive strength and flowability of AAM proportionally to the increase in R content. Experimental and statistical analysis reveal that curing in an oven at 60°C significantly optimizes compressive strength by approximately 50.52%. It is worth noting that this curing method of RAAM has demonstrated superior economic and environmental benefits compared to OPC mortar. The study highlights the strong potential of RAAM cured at 60°C or in a humid chamber, combining mechanical performance with reduced CO_2 emissions, as a sustainable and eco-friendly solution to replace traditional concrete.

1. Introduction

Geopolymers (GP) are increasingly attracting interest as a new class of sustainable construction materials, are subject to extensive research and practical applications [1, 2]. Contrary to ordinary Portland cement, which is estimated to contribute approximately 8% of global CO_2 emissions [3, 4], GPs are synthesized from aluminosilicate sources such as fly ash, slag, clay minerals, siliceous sand, or recycled aggregates, which are available locally [5, 6]. Their excellent mechanical strengths, durability, fire resistance, and low carbon footprint position them as next-generation binders in line with sustainable construction principles [7-9].

In parallel with the rise of geopolymers, waste production has continued to grow due to industrial development in recent decades. Among them, rubber waste represents a significant problem. It is estimated that around 1 billion tires reach the end of their lifespan every year, and this figure could reach 5 billion per year by 2030 [10, 11]. These huge volumes of non-biodegradable waste take up considerable space and pose environmental risks. The incorporation of alternative materials to replace natural aggregates in concrete could help reduce pressure on resources, as these aggregates account for 70% of the composition of concrete[12-14].

The incorporation of rubber in geopolymers presents a trade-off between decreasing mechanical performance and improving ductility [15]. Several studies in the literature have looked at the properties of geopolymers incorporating rubber aggregates Zhao, J., et al [16] as well as Qaidi, S.M., et al. [17] have shown that an increase in rubber content leads to a decrease in volumetric weight, as well as compressive, tensile, and flexural strengths of the material. Quantitatively, the presence of 10% rubber causes a 32% decrease in compressive strength. Researchers investigated the partial replacement of sand with crumb rubber (up to 20%) in fly ash-based geopolymer concrete. This substitution, according to Park et al.[18] led to a 35% decrease in compressive strength. However, the increased rubber content also enhanced the material's ductility. Similarly, Athira et al [19], partially substituted fines with rubber particles (0% to 20%) in fly ash and slag-based geopolymers, resulting in improved energy absorption at the expense of mechanical strength. Valente et al [20], highlighted enhanced interfacial compatibility between rubber aggregates and alkali-activated geopolymers, leading to improved porosity, flexural and toughness properties, albeit with compressive strengths consistently lower than equivalent Portland concretes. Parmender Gill et al . [21] demonstrated that geopolymer specimens with crumb rubber substitution exhibit up to a 17% reduction in compressive strength. Additionally, adding of Ordinary Portland cement improves microstructural integrity, but exposure to acid results in surface disintegration. Furthermore, optimal reinforcement with glass fibers reduces acid permeability, while the addition of steel fibers enhances both compressive and flexural strength. Abdullah et al.[22] studied the effects of incorporating rice husk ash (RHA) on the characteristics of lightweight geopolymer concrete, along with the addition of waste tire aggregates (WTA). The inclusion of WTA also resulted in a decrease reduction in density and compressive strength, with a further decrease in the thermal conductivity coefficient when WTA replaced 50% of the pumice aggregate.

In addition, various curing methods are commonly used for GPC, including ambient temperature curing, autoclave or steam curing, oven curing, and water curing. These processes aim to create the necessary conditions for the geopolymerization reaction, and to promote the development of the desired properties of the concrete [23, 24]. Liu et al. [25] have shown that GGBS content is crucial for mechanical properties, with better performance under thermal curing conditions. Accurate prediction models have been established for compressive strength. Specimens under optimal curing conditions exhibited a dense microstructure and characteristic hydrated gels.

Previous work by Luhar,S et al. [26], has demonstrated the effectiveness of high temperature curing (from 60 to 90°C) for a period ranging from 24 to 72 hours in improving the strength of GPs. Additionally, Park, Y., et al. [18], have highlighted the effectiveness of steam curing (in an autoclave) of GPs at a temperature of 46°C for 7 days. The study conducted by Rajendran and Akasi [27] revealed that oven curing is about 56% more effective than steam curing in terms of enhancing the strength of geopolymer concrete. Furthermore, Luhar, S. et al. [28], have indicated that a curing duration of 48 hours provides optimal compressive strength performance of rubber GPCs.

Expanding the study on the integration of rubber aggregates from used tires into AAM matrices represents a significant advancement towards more sustainable construction. This innovative approach aims to reduce environmental impact by incorporating recycled materials while enhancing concrete properties. What makes this study unique is the incorporation of recycled rubber fractions into AAMs, with the goal of designing concrete mixes that use a low carbon binder while improving characteristics such as lightness, mechanical strength, thermal and acoustic insulation, as well as durability. Based on previous research, a significant gap has been identified: the absence of studies investigating the synergistic effect between the presence of tire waste and the curing mode on AAM properties.

In this study, thoroughly investigate the effects of different proportions of rubber aggregates partially substituting mineral sand at volume fraction of (0%, 10%, 20%, and 30%) on the fresh and hardened properties of slag-based AAM. It also considers the impact of different curing modes, including air curing, chamber curing, or oven curing. The objective of this research is to mitigate the potential strength reduction in rubber-substituted AAMs while employing eco-friendly and cost-effective curing methods. To assess the correlation between the different parameters studied, an analysis of variance (ANOVA) was conducted using JMP software[29]. By conducting a comprehensive analysis of fundamental mechanics and bonding interactions, this research aims to facilitate wider adoption of oven-cured rubber-substituted AAM composites as alternatives to ordinary Portland cement concretes. The complete set of experimental data allows for a quantitative how these critical parameters influence on key performance measures of recycled rubber-substituted AAM composites.

2. Materials and Methods

2.1. Materials

In this study, Ground Granulated Blast Furnace Slag (GGBS) was used as precursor in the production of alkali-activated mortars (AAM). The GGBS was sourced from the El Hadjar steel complex located in Annaba, Algeria. The microstructures of GGBS were analyzed using the X-ray diffraction (XRD) technique, and the resulting phases are illustrated in Fig.1. As shown in Fig. 1, the calcite compounds with an amorphous structure demonstrate significant peaks. According to a previous study [30], the incorporation of GGBS was found to have a positive effect on the formation of calcium silicate hydrate (CSH) gel.
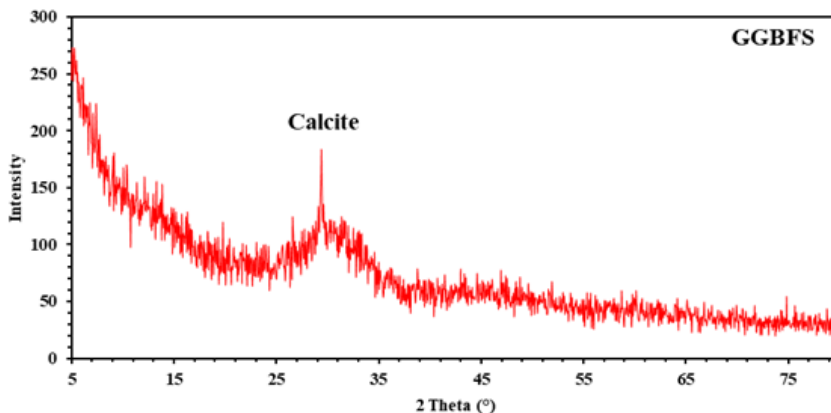
Fig. 1. X-ray diffraction of GGBS

This gel plays a crucial role in filling voids within the concrete matrix, thereby increasing the concrete's density. Figure 2 displays the particle size distribution and SEM image of GGBS. Its physical properties and chemical composition are detailed in Tables 1 and 2, respectively.

(a)   (b)
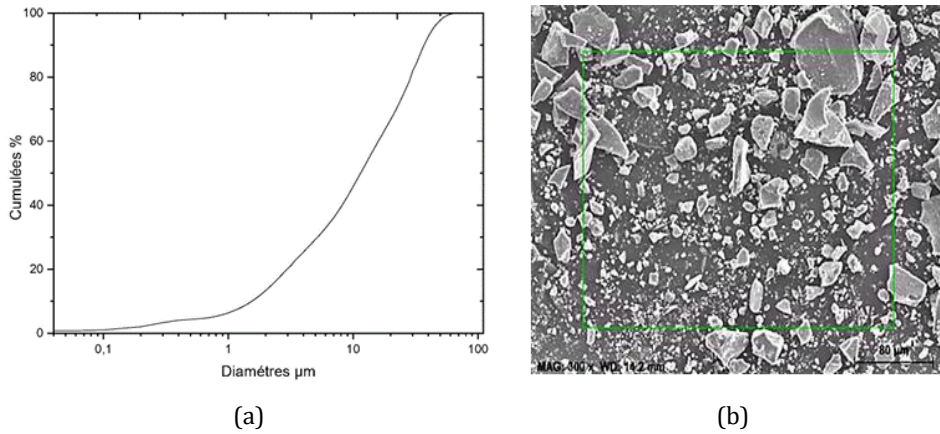
Fig. 2. (a) Particle size distribution measured by laser granulometry and(b) SEM image of GGBS

Table 1. Physical properties of sand GGBS and rubber particles

Properties	Sand	GGBS	R
Absolute density (g/cm^3)	2.6	3.08	0.93
Fineness Modulus	2.2	—	—
Water Absorption (%)	2.7	—	0.7
Apparent density (g/cm^3)	1.7	1.4	0.6
Blaine surface area (m^2/kg)	—	4155	—

Table 2. Chemical compositions of GGBS.

Specimens	SiO_2	AL_2O_3	F_2O_3	CaO	MgO	SO_3	K_2O	Na_2O	LOI
GGBS	35.34	7.52	6.75	38.50	3.28	0.43	0.59	0.2	1.03

For the preparation of geopolymer AAM, two different activators, namely sodium hydroxide (NaOH), with 99% of purity and sodium silicate (Na_2SiO_3) were commonly used as alkali activators. A 10 M NaOH solution was prepared by dissolving pellets in tap water and allowing them to rest for 24 hours before casting.

(a)   (b)   (c)

(d)   (e)

Fig. 3. Materials used in this study: (a) GGBS, (b)rubber, (c) river sand, (d) Na_2SiO_3
solution and (e) Solid NaOH

Additionally, a commercial Na_2SiO_3 solution was utilized in the process. The activators
employed in this study are illustrated in Figure 3, and their properties are detailed in
Table 3.

Table 3. Properties of activators

	Density (g/cm^3)	SiO_2 (wt%)	Na_2O (wt%)	H_2O (wt%)
NaOH powder	2.14	—	—	—
Na_2SiO_3 solution	1.53	29.8	14.43	55.77

The investigation employed two types of aggregates: natural river sand and rubber
particles. The river sand had a fineness modulus of 2.2 and was dried prior to use. Fig.4
illustrates the particle size distribution within the sand sample. The rubber particles,
sourced from discarded tires, had a size of 3 mm (as shown in Fig. 4). Table 1 provides the
physical characteristics of these aggregates, while Figure 4 visually represents the
aggregates used in the study.
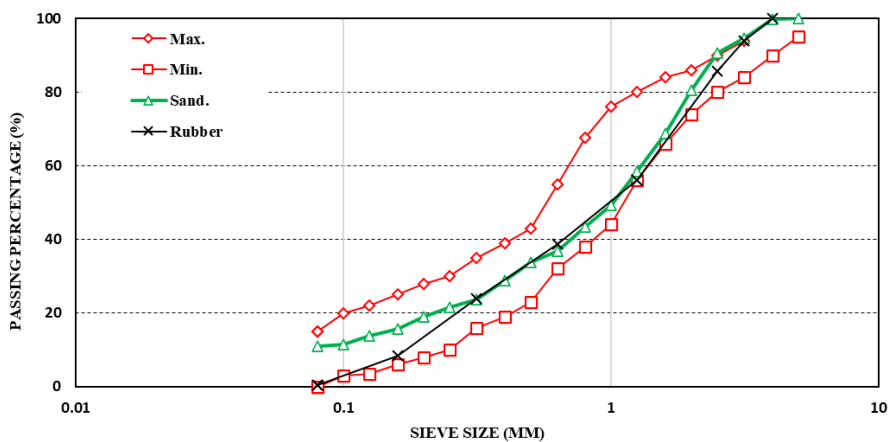
Fig. 4. Particle size distribution of natural sand and rubber

2.2. Rubber Treatment and Preparation of AAM Samples

Based on previous studies[31, 32], the activator solution was prepared by combining a 10M NaOH solution with Na_2SiO_3. The mixing process was carried out for 5-7 minutes. This activator solution was then kept at room temperature until the final mixing process. Furthermore, to evaluate the impact of rubber particles on the performance of AAM, sand was substituted with waste rubber particles at volume ratios of 0%, 10%, 20%, and 30%. The pretreatment of rubber particles involved washing them with tap water and then treating them with a NaOH solution. The rubber particles were initially rinsed with water to remove any impurities adhering to their surfaces. Subsequently, the particles were air dried for 48 hours at room temperature. After drying, the rubber particles were immersed in 5% NaOH solution at a temperature of 25°C for 24 hours. This NaOH treatment has been reported in a previous study to enhance the adhesion between rubber and other concrete ingredients [33]. Following the NaOH treatment, the rubber particles were washed multiple times to remove any remaining traces of NaOH from their surfaces. Finally, the pretreated rubber particles were dried at room temperature (60°C) for 48 hours. This pretreatment setup has been utilized in a previous study [34] and has demonstrated its effectiveness in achieving the desired results. Fig. 5 illustrates an organizational chart summarizing the processing steps for the different pretreatment methods of rubber particles.

The solid particles (GGBS, sand and rubber particle) were mixed for 3 minutes to ensure a higher level of homogeneity in the AAM. Subsequently, the activator solution was mixed with the solid particles for 2 minutes, blending the alkali solution and binder portion. Table 4 summarized the detailed compositions of all the mixes.

Fig. 5. The method used for processing treatment of rubber particles

The fresh mixtures obtained were poured into 25 mm cube molds in two separate layers, and each layer was compacted by applying 25 drops from a jolting table to remove air voids. After that, the specimens were subjected to three different curing modes. In the first curing mode (CM01), the molds containing the AAM samples are placed in an open-air chamber with an ambient temperature of 20°C and a relative humidity of 50% for 24 H. For the second curing method (CM02), the molded specimens were placed in an oven and maintained at a temperature of 60°C for a duration of 24 H.
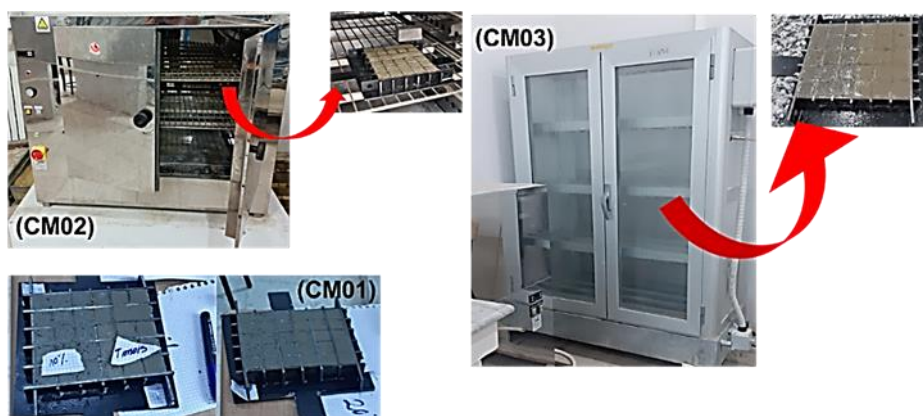
Fig. 6. Curing methods used for 24h, (CM01) an open-air chamber cured, (CM02) oven cured (CM 03) a humid room cured

In the third curing mode (CM03), the molded specimens were transferred to a humid room with a relative humidity (H) of 90% and an ambient temperature of 20°C. They were kept in this environment for 24 H. After curing method, the AAM were de-molded and placed in the laboratory at 20°C chambre until the testing age. Fig.6 shows the different curing methods employed in this study.

Table 4. Mixture proportions of AAM

Mix proportions (unit weight: Kg/m^3)					
Mixture	GGBS	Sand	Rubber	NaOH	Na_2SiO_3
CAAM	149	372	---	22	67
AAM-10R	149	335	13	22	67
AAM-20R	149	298	26	22	67
AAM-30R	149	261	39	22	67

Note: CAAM control Alkali-Activated Mortars without rubber, AAM-10R: Alkali-Activated Mortars with 10% rubber, AAM-20R: Alkali-Activated Mortars with 20% rubber, AAM-30R: Alkali-Activated Mortars with 30% rubber.

2.3. Experimental Procedure

2.3.1 Fluidity Test

To evaluate the workability of fresh AAM mixtures, a jolting table test was conducted following ASTM C1437 [35]. A cone-shaped container (dimensions in Fig.7a) was placed on the table and filled with the mixture. The mixture was then jolted 25 times, and its diameter was measured at two perpendicular points. The final result was reported as the average of these measurements.

2.3.2 Density

According to ASTM C642-13 [36], following the demolding process, the hardened density of AAM was determined using Equation (1):

$$\rho_r = \frac{m_r}{v_t} \qquad (1)$$

Equation 1 defines hardened density (ρ_r) as the ratio of a hardened specimen's mass (m_r) to its total volume (V_t). This volume is calculated by multiplying the length, width, and height of the cubic specimens. To ensure accuracy, each specimen's side length was measured six times at different locations and averaged. The AAM's final density is calculated by averaging the hardened densities of all six specimens.

2.3.3 Compressive Strength

According to the NF EN 196-1 standard [37], the compressive strength of AAM was measured using 25 mm size cubes. The testing was carried out using a hydraulic compression testing machine with a maximum capacity of 3000 kN, as depicted in Fig.7b.

2.3.4 Total Water Absorption

According to the EN 1015-18 standard [38], the water absorption test was conducted for all AAM and RAAM specimens. The aim of this test is to measure the water absorbed by the mortars over a 24-hour period. Water absorption is a vital factor for assessing and predicting the durability of building materials. [15] To determine the total water absorption of AAM, three cubes from each series were subjected to oven drying at a temperature of 85°C for 24 hours until a constant mass was achieved.

(a)

(b)

Fig. 7. Test equipment used, (a) flow test, (b) compression testing machine

The weight of the cubes after drying, recorded as the initial weight, was then compared to the saturated surface dry weight obtained after the AAM cubes were soaked in water for 24 hours or more at atmospheric pressure. The water absorption of the specimens was reported as the percentage increase in weight. The choice of an 85°C drying temperature was made to avoid potential disruptions in the microstructure of the AAM specimens and to ensure accurate water absorption values.

3. Results and Discussions

Table 5 presents a comprehensive summary of all the experimental findings. It is worth noting that the recorded errors for each composition did not exceed 3%. This indicates that the modeling of the responses, specifically the compressive strengths at 28 days (CS_{28}), was successful, as the errors remained within an acceptable range.

Table 5. The experimental results

Curing methods	Mixture	R (g)	Flow table (mm)	Fresh Density (Kg/m^3)	Hardened Density (Kg/m^3)	CS_{28} (MPa)	WA (%)
CM01	CAAM01	0	195	2341	2387	35.36	7.361
	AAM-10R	50.92	179.5	2272	2354	30.32	7.77
	AAM-20R	101.84	172	2176	2238	23.07	8.15
	AAM-30R	152.76	155	2129	2156	17.78	9.13
CM02	CAAM 02	0	195	2341	2403	53.24	6.42
	AAM-10R	50.92	179.5	2272	2370	39.74	7.34
	AAM-20R	101.84	172	2176	2322	34.60	7.86
	AAM-30R	152.76	155	2129	2173	23.72	8.29
CM03	CAAM 03	0	195	2341	2395	44.95	7.03
	AAM-10R	50.92	179.5	2272	2367	38.96	7.43
	AAM-20R	101.84	172	2176	2309	32.98	8.24
	AAM-30R	152.76	155	2129	2212	27.15	8.57

3.1. Flow Table Test Results

In order to determine the workability of various AAM mixes, flow table tests were conducted in compliance with the ASTM C1437 23 [35] standard. The flowability test results are shown in Fig.8. The CAAM exhibited the highest level of flowability among all the mixes, with a maximum measurement of 195 mm.
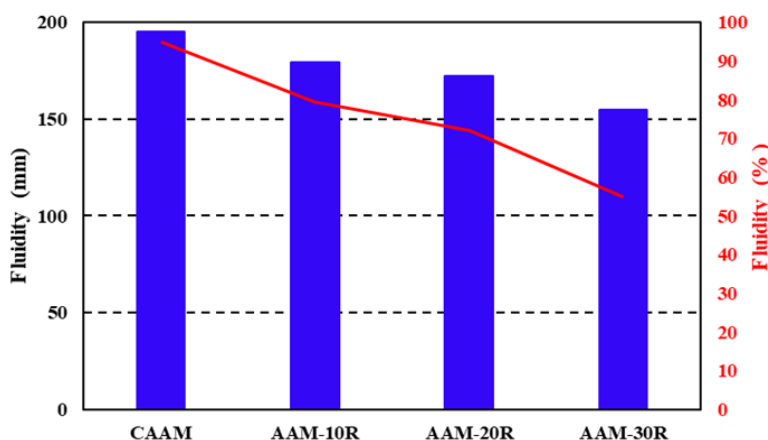
Fig. 8. Effects of rubber content on RAAM fluidity

The results showed the impact of rubber content on the fluidity of the rubber alkali-activate mortar (RAAM). It can be observed that as the rubber content increases, the fluidity of the RAAM decreases. When the rubber replacement levels are increased to 10%, 20%, and 30%, the fluidities of the RAAM mixtures decrease by 8%, 12%, and 20%, respectively, compared to the CAAM. This finding aligns with previous research on RAAM [9, 39, 40], which has shown that incorporating rubber particles can notably affect the

fluidity of geopolymer mixtures. As the rubber content increases, the fluidity decreases, reinforcing the understanding of the connection between rubber content and fluidity in geopolymer systems. The decrease in workability observed when incorporating rubber in AAM can be attributed to several factors. Firstly, the rough surface of rubber particles increases friction between the rubber particles and the other components of the AAM, resulting in reduced workability [41]; Secondly, the hydrophobic nature of rubber particles leads to increased air entrapment, further decreasing the flow resistance of the mixture. This can contribute to the reduction in workability of RAAM. Lower workability is also attributed to reduced friction, hindered flow of large rubber particles, and the texture of small rubber aggregates [41]. The low density of rubber particles may further contribute to the decrease in workability. Furthermore, incorporating waste rubber aggregates as aggregates in lightweight geopolymer concrete diminishes workability, consequently increasing the proportion of trapped air bubbles [42]. However, it is interesting to note that the rubber content has a lesser impact on the fluidity of RAAM. This implies that pretreatment with NaOH might have enhanced the interface performance of the rubber, thereby offsetting the adverse impacts of increased rubber content on fluidity [43]. The improved interface performance could be attributed to the hydrophilic nature of the rubber particles, which can serve as a standard for assessing the enhancement of rubber-cementitious materials [44]. Overall, the workability of all the AAM mixes fell within the acceptable range for their application in construction practices.

3.2. Density

Table 5 and Figure 9 illustrate the impact of rubber content on the fresh and hardened densities of the AAM specimens. The findings indicate that the addition of rubber particles in AAM leads to a decrease in its fresh density, and this reduction becomes progressively more pronounced with higher rubber content.
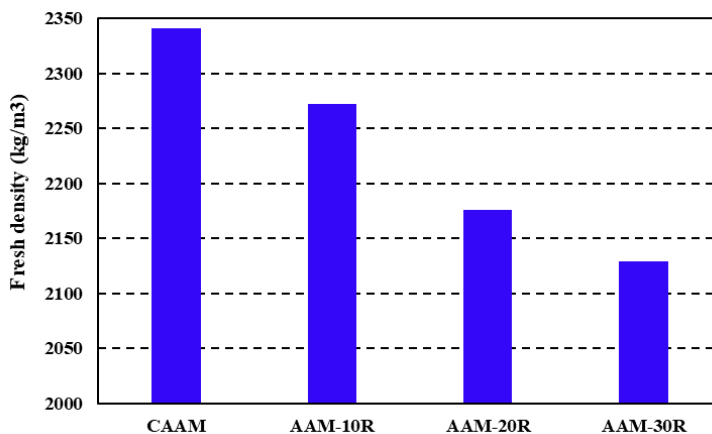
Fig. 9. Fresh AAM density of various mixes

As shown in Fig. 9, the fresh density of the RAAM ranged from 2272 Kg/m^3 to 2138 Kg/m^3, while the hardened RAAM densities for CM01, CM02 and CM03 varied from 2354-2156 Kg/m^3, 2370-2173 Kg/m^3 and 2367-2212 Kg/m^3 respectively (see table 5) , and were slightly lower than that of the control mix (without rubber), which is consistent with an earlier study [45, 46]. For example, the fresh densities of the AAM with 10%, 20%, and 15% rubber were reduced by 2.9%, 7.4%, and 10.0%, respectively, in comparison to those without rubber. Using 30 % R decreases the hardened density of AAM to about 212, 230 and 183 Kg/m^3 for CM01, CM02 and CM03, respectively. This reduction in density

contributes to improved thermal and sound properties of the composite. It is widely acknowledged that rubber has a lower density compared to river sand [42]. The average specific gravity of rubber particles is approximately 0.93, which is 2.6 times lower than that of sand. Additionally, rubber particles serve as solid hydrophobic air-entraining agents [47], meaning they introduce more air into the alkali-activated mixture.

3.3. Relationship Between 28-Day Compressive Strength and Water Absorption

Linear regression analysis was employed to investigate the correlation between the 28-day compressive strength and water absorption of AAM. The results of this analysis are presented in Fig.10. Linear regression is a statistical technique used to establish the relationship between two variables. By fitting a linear equation to the data, it becomes easier to comprehend the impact of different parameters. The linear equations developed in this study provide basic insights into the influence of various factors.

$$y = -12.777x + 133.17$$
$$R^2 = 0.8864$$
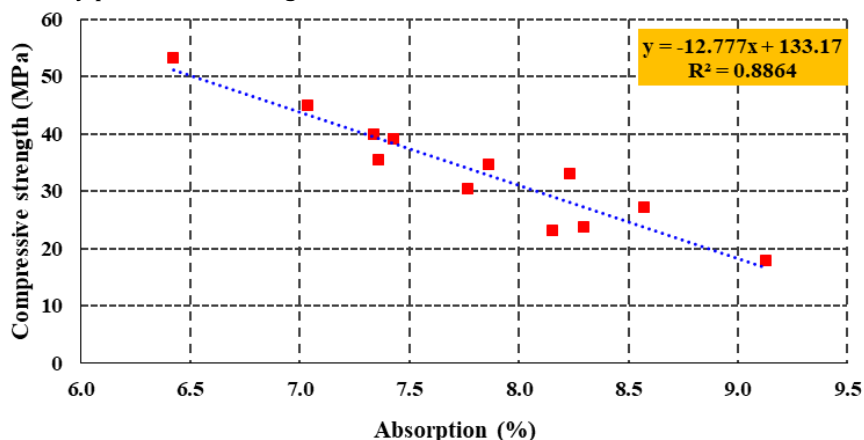
Fig. 10. Relationship between 28-day compressive strength and water absorption of various mixes

The average correlation value (R^2) for the linear fitting curve of compressive strength and water absorption was approximately 0.88, indicating a strong correlation between the variables. The positive slope observed in the graph indicates a direct relationship between compressive strength and water absorption, implying that as water absorption increases, the compressive strength tends to increase as well. This finding aligns with the theory that reducing the presence of pores enhances the resistance of cementitious materials. Notably, Kirgiz et al. [48] also reported similar results, further validating this theory.

3.4. Statistical Analysis Results

Various designs, as described by Dean et al. [49] and Lawson [50], can be employed to investigate the relationships between factors and responses. In the experimental program, the focus was on evaluating the compressive strength and water absorption of AAM, while also studying the impact of curing methods and the incorporation of crumb rubber on these properties[51, 52]. The analysis of these factors was carried out using the "JMP 16" software [53].

3.4.1 Analysis and Outcomes of The Variance Within The Model

The ANOVA analysis presented in Figs 11 and 12 partitions the overall variability of the dependent variables, namely compressive strength, and water absorption, into two components: one attributed to the regression and the other to deviations around the fitted

model. The R-squared statistic (RSq), calculated by comparing the model sum of squares to the total corrected sum of squares, indicates that the model explains approximately 98% and 96% of the variability in compressive strength and water absorption, respectively.

(a)   (b)
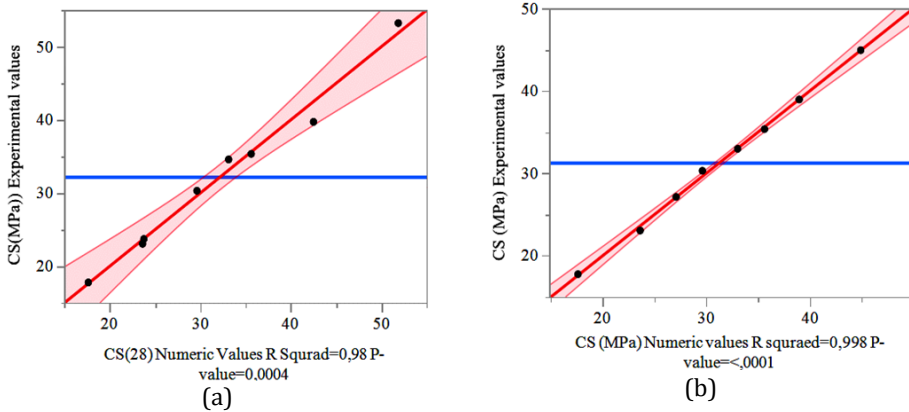
Fig. 11. Compressive Strength Actual by Predicted Plot for AAM cured in oven (CM02)
and cured in a humid room (CM03)

The mean squared error (EMSE) serves as an estimate of the variance of the deviations around the model, obtaining values of 0.222 to 3.134 and 0.04617 to 0.05229 for compressive strength and water absorption, respectively. The fact that the P value is less than 0.0004 for both compressive strength and water absorption demonstrates that the model is statistically significant, indicating a meaningful relationship between the predictors and responses.

(a)   (b)
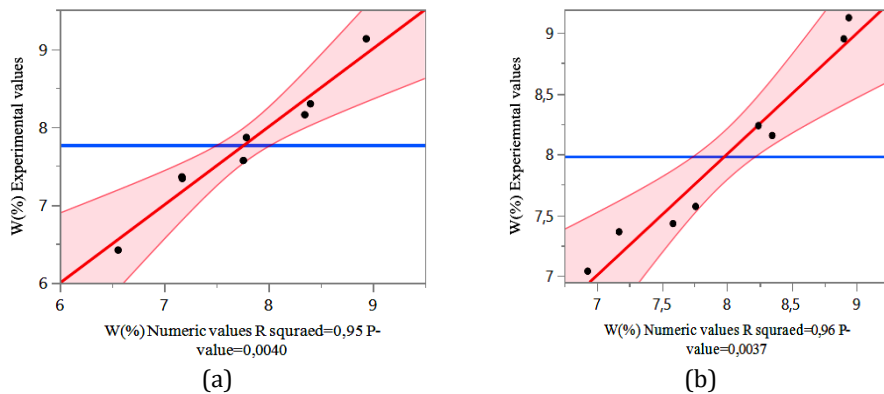
Fig. 12. Water absorptions at 28 days, actual by Predicted Plot (a) for AAM cured in oven (CM02) and (b) for AAM cured in a humid room (CM03)

Table 6 presents the ANOVA analysis for all modeled responses. The Fisher test, based on the Fisher test distribution, allows us to evaluate the statistical significance of these models, indicating their overall importance. In this study, the Frisher rations for both curing modes CM02 and CM03 are 0001 and 0.0004 for CS_{28}, 0.0004 and 0.0040 for WA respectively. With a 90% confidence interval, signifying a notable level of significance. The probability values (P-values) exceeding the F-statistic (Prob. > F) were all below 5% for every model, suggesting the presence of at least one factor with a statistically significant impact in each model. This suggests that the effect factors considered in the models have a notable impact on the responses.

Table 6. ANOVA (Analysis of Variance) for the derived models

	Source	Degree of freedom	Sum of squares	Mean square	F -ratio
CS_{28}	Model	3	531.83018	177.277	798.8634
	Error	4	0.88764	0.222	Prob. > F
	Total	7	532.71782		<.0001*
CS_{28}	Model	3	869.45871	289.820	92.4891
	Error	4	12.53422	3.134	Prob. > F
	Total	7	881.99293		0.0004*
WA	Model	3	3.9250779	1.30836	28.3367
	Error	4	0.1846873	0.04617	Prob. > F
	Total	7	4.1097653		0.0037*
WA	Modèle	3	4.2770621	1.42569	27.2663
	Erreur	4	0.2091502	0.05229	Prob. > F
	Total	7	4.4862123		0.0040*

According to the Table 7, it is clear that the contributions of each factor, rubber particle (R %), relative humidity (H%), and temperature (T °C), along with their interactions, to the responses are significant. The significance of each coefficient was assessed using the criterion P ≤ 0.05, and it was observed that the effects of the factors R %, H%, T°C, and their interactions on the responses are highly significant.

Table 7. Effect test

	Model term	Estimation	Standard Error	t ratio	Prob. > |t|
CS_{28} CM02	Intercepts	31.320875	0.166354	188.28	<.0001*
	R (%)	-8.95425	0.223188	-40.12	<.0001*
	H (%)	4.68675	0.166354	28.17	<.0001*
	R (%)×H (%)	0.047025	0.223188	0.21	0.8434
CS_{28} CM03	Intercepts	32.230063	0.62594	51.49	<.0001*
	R (%)	-11.52769	0.839786	-13.73	0.0002*
	T(°C)	5.5959375	0.62594	8.94	0.0009*
	R (%)×T(°C)	-2.526412	0.839786	-3.01	0.0396*
WA CM02	Constante	7.983825	0.07597	105.09	<.0001*
	R(%)(0.30)	0.93369	0.101925	9.16	0.0008*
	H(%)(50.90)	-0.069925	0.07597	-0.92	0.4094
	R(%)*H(%)	0.05064	0.101925	0.50	0.6454
	Constante	7.7674125	0.080845	96.08	<.0001*
WA CM03	R(%)(0.30)	0.9023925	0.108465	8.32	0.0011*
	T(°C)(20.60)	-0.286413	0.080845	-3.54	0.0240*
	R(%)*T(°C)	0.0192075	0.108465	0.18	0.8680

3.4.2 Expression for predicting the values of compressive strength and water absorption

Based on the conducted statistical analysis, the following prediction expressions, represented by Eqs. (2)-(5), were derived to estimate the values of compressive strength

and water absorption in relation to the rubber incorporated (R%) and curing methods (oven cured (CM02) and a humid room cured (CM03)).

The compressive strength of, which were cured in CM02, can be described with the following expression:

$$CS(28\ days) = 32.23 - 11.527.\left(\frac{R(\%) - 15}{15}\right) + 5.595.\left(\frac{T(C) - 40}{20}\right)$$
$$- .5264.\left(\frac{R(\%) - 15}{15}\right).\left(\frac{T(C) - 40}{20}\right) \tag{2}$$

The compressive strength of AAM, which were oven cured CM03, can be described with the following expression:

$$CS(28\ days) = 31.32 - 8.954.\left(\frac{R(\%) - 15}{15}\right) + 4.686.\left(\frac{H(\%) - 70}{20}\right)$$
$$+ 0.047.\left(\frac{R(\%) - 15}{15}\right).\left(\frac{H(\%) - 70}{20}\right) \tag{3}$$

The expression for water absorption (%) of AAM cured in CM02 can be given as follows:

$$W(\%) = 7.767 + 0.9023.\left(\frac{R(\%) - 15}{15}\right) - 0.286.\left(\frac{T(C) - 40}{20}\right)$$
$$+ 0.0192.\left(\frac{R(\%) - 15}{15}\right).\left(\frac{T(C) - 40}{20}\right) \tag{4}$$

The expression for water absorption (%) of AAM cured in CM03 can be given as follows:

$$W(\%) = 7.983 + 0.9336.\left(\frac{R(\%) - 15}{15}\right) - 0.0699.\left(\frac{H(\%) - 70}{20}\right)$$
$$+ 0.0506.\left(\frac{R(\%) - 15}{15}\right).\left(\frac{H(\%) - 70}{20}\right) \tag{5}$$

3.4.3 Compressive Strength Results Analysis

The different types of graphs from the analysis of the results of the compressive strength (CS) at 28 days, taking into account the factors of rubber particles content (%) and curing methods are presented in Fig 13, 14, 15 and 16. The compressive strength is assessed by the average force of three cubic samples (Table 5). For the control samples using the CM01 curing method, a maximum compressive strength (CS) of 35.37 MPa was observed at 28 days. With the partial substitution of sand by rubber particles, a significant decrease in the CS of AAMs was observed. AAM-10R displayed a reduced strength of 14%, this is equivalent to. 30.32 MPa, compared to CM01. Similarly, AAM-20R and AAM-30R recorded respective strength losses of 34% (23.07 MPa) and 49% (17.78 MPa). The CS of the samples subjected to CM02 and CM03 curing methods was measured at 53.24 MPa and 44.95 MPa respectively. The results of partial substitution of sand by rubber particles in AAMs showed a downward trend in CS, similar to that observed with CM01. For CM02, AAM-10R revealed a 25% strength reduction, reaching 39.74 MPa, while for CM03, the reduction was 13%, 38.96 MPa. In addition, AAM-20R and AAM-30R showed more pronounced strength decreases: For CM02, the losses were 35% and 55%, while for CM03, they were 26% and 39%. These results reveal clear trends regarding the impact of sand substitution by rubber particles on the compressive strength of AAMs. It is evident that the integration of rubber negatively affects compressive strength, regardless of the curing method used (CM01, CM02, or CM03). This loss of performance varies according to the percentage of substitution and the curing method. Moreover, this decrease in load bearing capacity can be attributed to crucial factors such as reduced density and elasticity of rubber, increased porosity due to trapped air, and hydrophobicity of rubber, all of which contribute to decreased compressive strength [54] [55] [28].
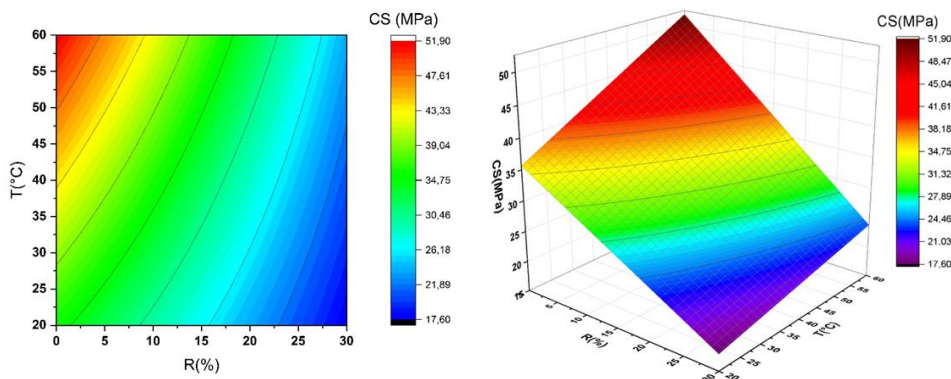
Fig. 13. Iso-response analysis of 28-Day compressive strength in RAAM CM02
subjected to oven curing

Re-focusing the analysis on the impact of curing methods, makes it clear that they are key in optimizing the CS strength of AAMs. Specimens treated with the CM02 method, oven-cured at 60°C without adding rubber particles, demonstrated a marked improvement in CS compared to other techniques. After 28 days, CM02 shows a significant increase in CS of 50.52% compared to CM01 and 18.44% compared to CM03. These data highlight the effectiveness of 60°C curing without rubber particles to increase the strength of AAM samples, this observation is in total agreement with the work of Mustafa Al Bakri et al. [56] who identified 60°C as the optimal curing temperature for geopolymer specimens. Their research also reveals that geopolymers cured at high temperatures suffer from a lack of moisture necessary for optimal strength development. Liu et al. demonstrated the significance of GGBS content in influencing mechanical properties, particularly showing improved performance under thermal curing conditions. They developed precise prediction models for compressive strength. Specimens cured optimally displayed a dense microstructure and distinctive hydrated gels. In a study by Joseph and Mathew [57], geopolymer concrete specimens were cured at different temperatures, ranging from 30 °C to 100 °C. The results showed that the compressive strength of the concrete increased significantly with higher curing temperatures.

(a)

(b)
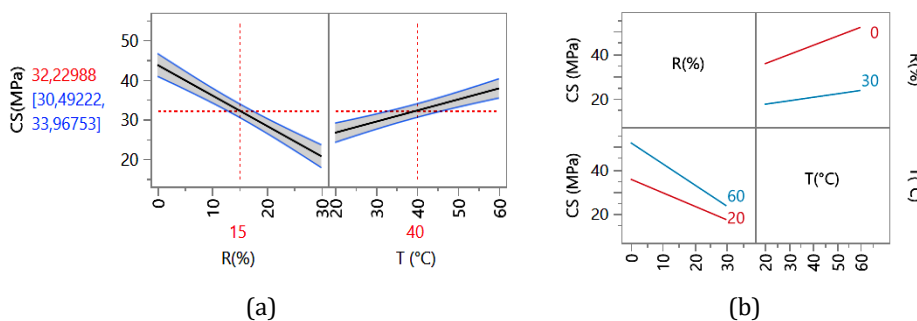
Fig. 14. (a) Main effects plot (b) interaction plot of the 28-day compressive strengths
for AAMR oven cured CM02

Figures 14 and 16 present the main effects plots on the 28-day CS response of AAM, taking into account factors of rubber particles content (%), T (°C) and H (%). Analysis of the data presented in Table 7, together with the graphical visualizations in Fig14a and 16a, reveals the complex dynamics governing the 28-day CS of AAMs. The negative influence of rubber

percentage on CS is highlighted by negative coefficients of -11.52769 for CM02 and -8.95425 for CM03, underscoring an inverse proportional effect between CS and amount of R incorporated.
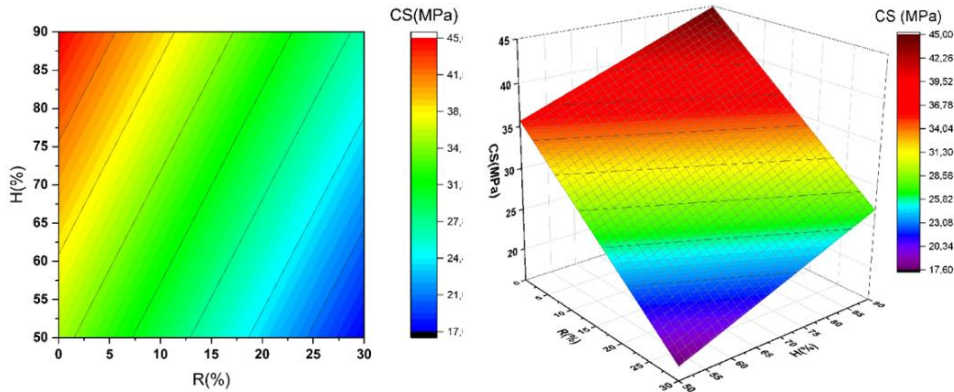
Fig. 15. Iso-response curves and surfaces illustrate the variations in 28-day compressive strengths for AAMR cured in a humidity room CM03

In parallel, a positive coefficient of +5.599375 for curing temperature (T in °C) indicates that increasing temperature promotes improvement in CS, up to an optimal point. This synergy is illustrated in Figure 14a for oven-cured AAM CM02, where rising T causes an increase in CS, while addition of rubber particles decreases it, a relationship that is graphically supported by the trends observed in the 14b interaction plot.

Figure 16a exposes the effects of rubber particles (%) and humidity (H%) on chamber-cured AAMs CM03. The decreasing CS with increasing rubber particles (%) is clearly visible in the downward curve of the plot. However, the 16b interaction plot reveals that the interaction between rubber particles (%) and H (%) does not have a pronounced impact on CS, deduced from the near-parallelism of the curves.

(a)

(b)
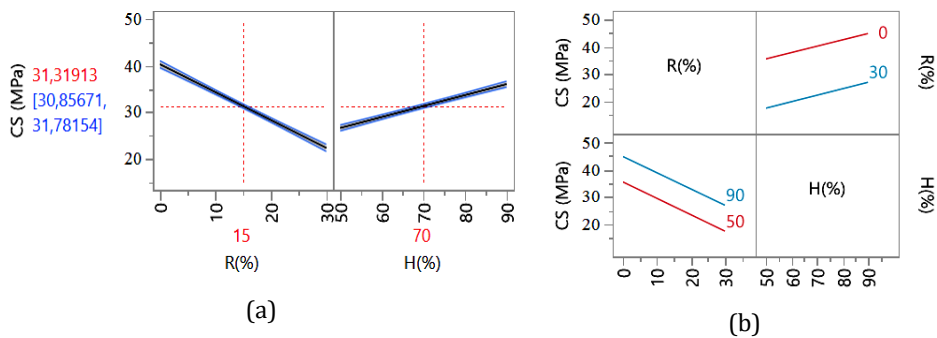
Fig. 16. Main (a) and Interactive (b) Drivers of AAMR Compressive Strength in Humidity Room CM03 (28-Day Analysis)

3.4.4 Water Absorption Results Analysis

The water absorption responses of AAM for CM02 and CM03 curing methods are illustrated in Figures 17, 18, 19 and 20. Figures 17 and 19 illustrate the response surface

curves and isometric plots of the 28-day water absorption (WA) of AAM as a function of the sand substitution rate by rubber particles, for the different curing methods studied.

Analysis of the data shows an upward trend in water absorption as the rubber proportion rises from 10% to 30%, regardless of the curing method used, oven-cured CM02 or chamber-cured CM03. Specifically, for CM02, water absorption increases from 7.34% to 8.29%, and for CM03, it rises from 7.43% to 8.57%, revealing a direct and proportional relationship between the increase in rubber particles content and the material's WA after 28 days.
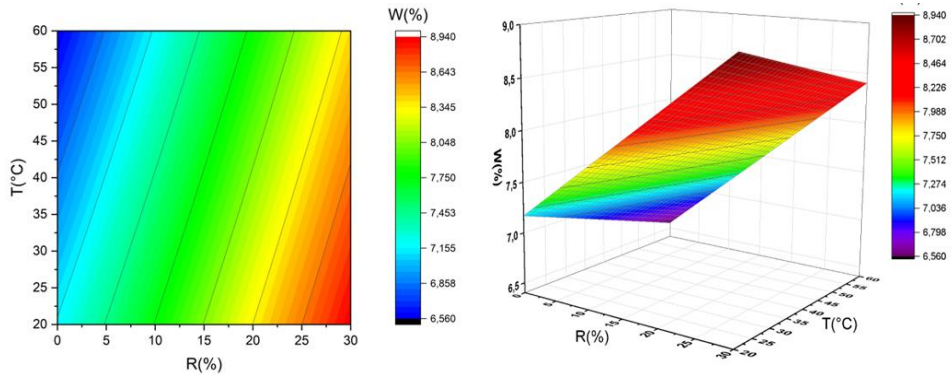
Fig. 17. Mapping the influence of process parameters on AAMR water absorption (28 Days) using iso-response analysis

According to Dehdezi et al. [58], weak bonding between the geopolymer and the rubber particles creates a poor interfacial transition zone (ITZ). This weak zone, in turn, increases the number of apparent pores in the material. These observations are validated by the coefficients presented in Table 7 and defined by Equations (4 and 5). The coefficients for rubber particles (%) are positive, with (+0.90) for CM02 and (+0.93) for CM03, confirming a positive correlation between the amount of rubber and the observed WA.

(a)   (b)
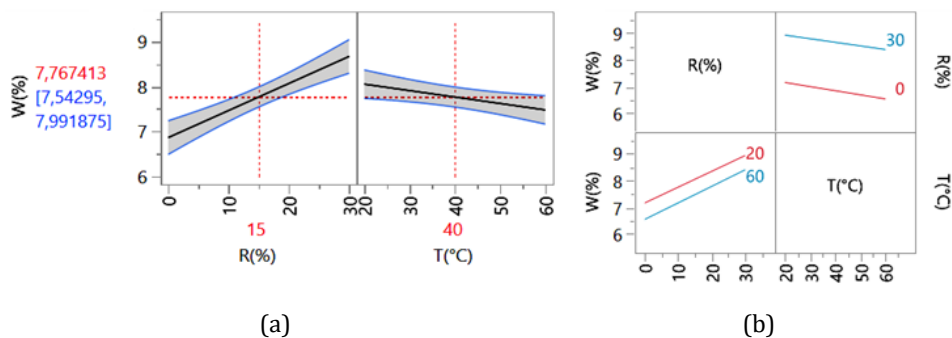
Fig. 18. AAMR Water Absorption (28-Day): Main (a) & Interaction Effects (b) (Oven Cured CM02)

The coefficients for temperature (T °C) and humidity (H %) are (-0.28) and (-0.08) respectively, indicating an inverse relationship between these parameters and water absorption suggesting that increases in temperature and humidity help reduce WA. This result highlights the overriding influence of rubber particle replacement rate and curing conditions on the hygral behavior of AAMs.
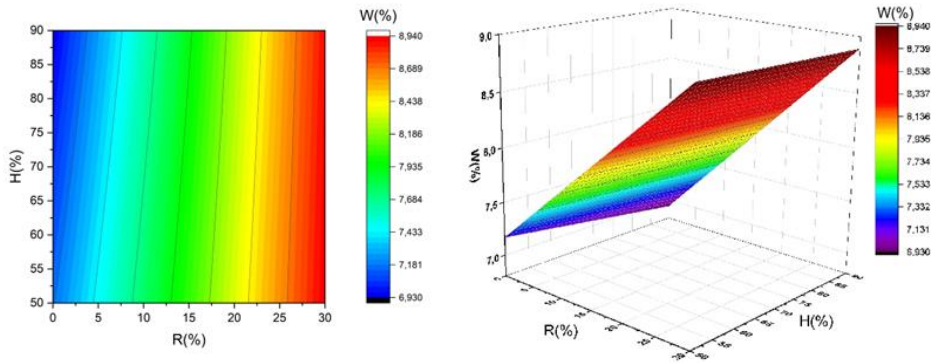
Fig. 19. Iso-response Modeling of AAMR water Absorption in Humidity Room CM03

Figures 18b and 20b present detailed interaction plots of the dynamics governing the 28-day WA of different AAM mixes. In oven-cured CM02 samples, the interaction plots display parallel behavior between the rubber particles content factor (%) and temperature (T°C), indicating an absence of marked synergy between these variables on water absorption. In contrast, the interactions in chamber-cured CM03 samples exhibit crossing curves, revealing a significant interdependence between the rubber particles content factor (%) and humidity (H%). This difference suggests that curing conditions significantly influence AAMs. Conversely, analysis of the results for AAM without rubber particles exposes a reduction in capillary absorption for the compositions subjected to CM02 curing with a respective decrease of 18% and 9% compared to the control compositions CM01 and CM02.

(a)

(b)
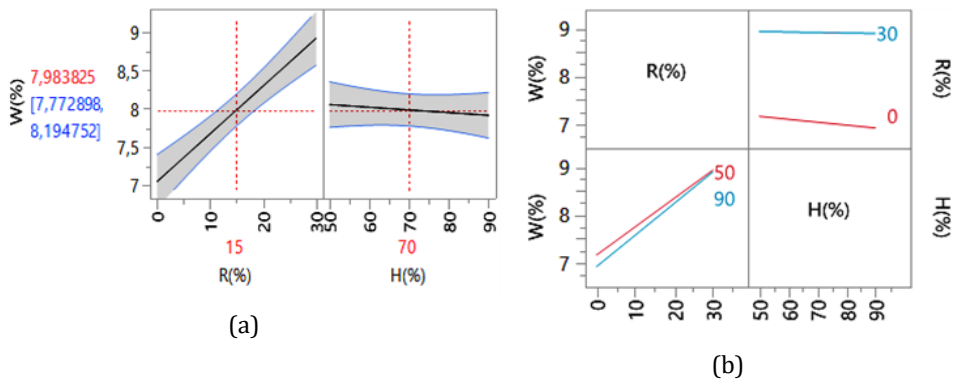
Fig. 20. Main (a) and interactive (b) drivers of RAAM water absorption in oven-cured CM02 (28-Day Analysis)

3.5. Economic and Ecological Analyses

In this section, we offer an assessment of the carbon dioxide emissions and conduct a financial analysis for the AAM blends formulated in this research. The aim is to assess the environmental and economic implications of substituting rubber particles with natural sand in the AAM compositions, which are subjected to various curing techniques. To quantify the RAAM's cost-effectiveness and environmental footprint, we employed two indices developed by Ma [59] (Equations 6 and 7).

$$C_P = \frac{Cost}{fc28} \qquad (6)$$

The cost-efficiency and environmental impact are calculated using a formula that considers the cost per unit of strength (C/$MPa), the total material cost per cubic meter (Cost), and the material's 28-day compressive strength (σ). The cost-efficiency and environmental impact are calculated using a formula that considers the cost per unit of strength (C/$MPa), the total material cost per cubic meter (Cost), and the material's 28-day compressive strength (σ).

$$E_P = \frac{embodied\ CO_2}{fc28} \qquad (7)$$

Embodied CO_2 per MPa (Ep ($kg/Mpa.m^3$)) and total embodied CO_2 (($kgCO_2$)/(kg)) were calculated for the AAM, considering its 28-day compressive strength (fc28) and local raw material costs in Algeria. These calculations also incorporated the embodied CO_2 data for the raw materials sourced from relevant research [16, 59, 60]. The findings from these calculations are detailed in Table 8.

Figure 21a and Table 9 present the calculated CP values for the AAM subjected to various curing conditions. Notably, the CP values for each AAM mixture exceed those of Ordinary Portland Cement (OPC). When comparing AAM mixtures without rubber, it's evident that the CP values of CAAM01 and CAAM03 are nearly double that of OPC, while CAAM02 and OPC exhibit only a slight difference in CP values. Additionally, incorporating rubber into RAAM results in an elevated CP value. This can be attributed to two primary factors: firstly, the adverse impact of rubber on the compressive strength of the mixture, and secondly, the higher cost associated with using rubber compared to natural aggregate. These factors collectively contribute to the observed increase in the CP of the RAAM.

Table 8. Cost and embodied CO_2 of raw materials.

Materials	Reel study Cost ($/kg$)	embodied $CO_2(kgCO_2/kg)$	
GGBS	0.035	0.067	[61]
Sand	0.029	0.005	[16]
Cement	0.12	0.830	[62]
Rubber	0.67	0.004	[59]
NaOH powder	4.06	1.915	[63, 64]
Na_2SiO_3 solution	0.56	0.650	[64, 65]
Water	0.00372	0.001	[16]
Energy	($/kwh$)	($kgCO_2$/kWh)	
Heating	0.28	1.08	[60]

Regarding the impact of curing methods on the CP values of RAAM, it was noted that the humidity curing method (CM03) demonstrated significant economic efficiency. This suggests that CM03 could be a viable option for real-world application in engineering projects, especially when compared to the preparation methods evaluated by CM02, which require more thermal energy (refer to Table 8). The E_P values for different RAAM mixtures are depicted in Fig. 21b. It is clear that AAM exhibits a higher level of environmental friendliness compared to OPC. While adding rubber increased the material's embodiedCO_2 per MPa (Ep), its inherently lower CO_2 intensity per unit mass compared to natural aggregate could offer an environmental benefit.
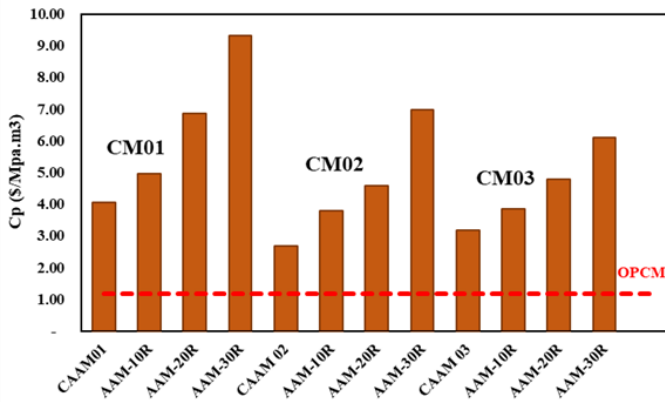
(a)
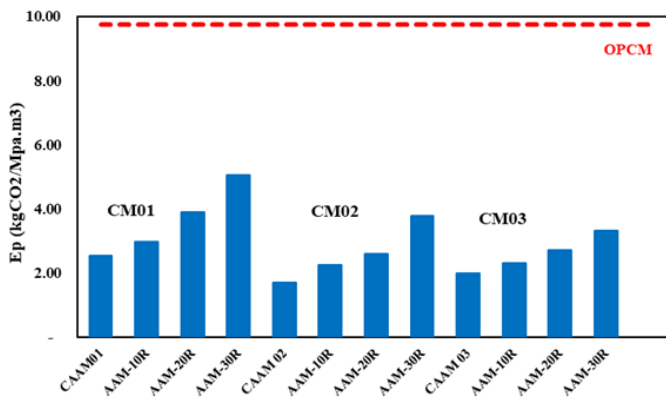
(b)

Fig. 21. (a) Cost efficiency and (b) environmental impact of curing methods on the AAM

Table 9. AAM cost efficiency and environmental impact

Curing methods	Mix	Compressive strength (Mpa)	Cp ($/Mpa. m^3)	Ep (kgCO$_2$/ Mpa. m^3)
	CAAM01	35.37	4.04	2.56
	AAM-10R	30.32	4.96	2.98
CM01	AAM-20R	23.07	6.85	3.91
	AAM-30R	17.78	9.32	5.06
	CAAM 02	53.24	2.68	1.70
	AAM-10R	39.74	3.79	2.27
CM02	AAM-20R	34.60	4.57	2.60
	AAM-30R	23.72	6.99	3.79
	CAAM 03	44.95	3.18	2.01
	AAM-10R	38.96	3.86	2.32
CM03	AAM-20R	32.98	4.79	2.73
	AAM-30R	27.15	6.11	3.31
	OPCM	30.00	2.19	9.75

However, this advantage was offset by the decrease in compressive strength caused by the rubber, leading to a negative impact on the RAAM's overall ecological index. In addition, incorporating rubber particles into the RAAM mixture led to an increase in the E_P value, indicating higher embodied CO_2 emissions. It is important to note that rubber has a lower carbon footprint when compared to natural aggregates. However, the reduction in compressive strength resulting from the use of rubber had an adverse effect on the ecological index of the RAAM, affecting its overall ecological performance. A significant finding emerged from the study, revealing that the E_P of RAAM was lower than that of OPCM. This discrepancy can be predominantly attributed to the substantial CO_2 emissions generated during cement production. This discovery highlights the imperative need to promote the advancement and application of RAAM as a strategy to mitigate environmental impacts, particularly by reducing embodied CO_2 emissions.

In terms of the influence of curing methods on the E_P values of RAAM, it was observed that the humidity curing method (CM03) exhibited notable economic efficiency. This indicates that CM03 holds promise for practical implementation in engineering projects, given the currently available preparation methods compared by CM02, which require more thermal energy (see Table 8). In terms of evaluating the embodied environmental impact, CM03 is identified as the most favorable choice for producing a cleaner AAM. It is subsequently followed by CM01, with CM02 being the least preferable option in terms of their respective environmental impacts. A comprehensive analysis of economics and environmental sustainability highlights CM03 as the preferred curing approach for RAAM. Furthermore, incorporating 5% rubber content proves ideal, meeting strength demands while unlocking significant economic and ecological benefits.

3.6 Synthesis of Discussion

The study provides a comprehensive analysis of the effects of rubber content on the properties of alkali-activated mortar (AAM), covering flowability, density, compressive strength, and water absorption. The results reveal that increasing rubber content decreases the flowability of AAM, with a reduction ranging from 8% to 20% in the flowability of RAAM mixes compared to CAAM. This decrease is attributed to increased friction between rubber particles and AAM components, increased air entrainment due to the hydrophobic nature of rubber, and lower density of rubber particles. However, pre-treatment with NaOH appears to enhance interface performance, mitigating the adverse effects of rubber content on flowability. Additionally, incorporating rubber reduces both fresh and hardened densities of AAM, with reductions of 2.9% to 10% in fresh density and 183 Kg/m^3 to 230 Kg/m^3 in hardened density for 30% rubber substitution levels. Curing methods significantly influence compressive strength, with higher curing temperatures generally favouring increased strength. However, a curing temperature of 60°C appears optimal for compressive strength development, with an increase of 50.52% compared to other curing methods. Furthermore, water absorption increases with higher rubber content, with increases from 7.34% to 8.29% for oven curing and from 7.43% to 8.57% for chamber curing. Economic and ecological analyses reveal that incorporating rubber increases costs and environmental footprint compared to natural sand, with a notable increase in costs per unit of compressive strength and carbon footprint. In summary, this study provides valuable insights for informed decision-making in construction practices, considering both performance and sustainability considerations.

4. Conclusions

Based on this study, it is concluded that:

- The results show a gradual decrease in compressive strength with increasing rubber particles content, indicating a negative correlation between rubber content and compressive strength.
- Curing methods have a significant impact on AAM properties, with 60°C oven curing (CM02) markedly improves compressive strength compared to other conditions.
- Flowability tests reveal that adding rubber particles reduces the flowability of AAM mixes, with decreases of up to 20%, highlighting the marked influence of rubber on the workability of the materials.
- The incorporation of rubber particles reduces the density of AAMs, thereby helping to improve the thermal and acoustic properties of the composite, while exhibiting a significantly lower average specific density than that of sand.
- A strong correlation ($R^2 \approx 0.88$) between 28-day compressive strength and water absorption was identified, suggesting that reduced porosity enhance the strength of cementitious materials. ANOVA analyses confirm the significant importance of the established models, with P values less than 0.05, indicating a significant relationship between predictors and responses.
- The incorporation of rubber increases the water absorption of AAMs in proportion to the substitution rate regardless of the curing method. In contrast, the absorption of control samples without rubber decreases with CM02 heat curing by about 18%.
- Economic and ecological analysis highlights that CM02 curing presents notable economic efficiency, suggesting significant practical application potential, in addition to being identified as the most favorable choice for producing environmentally cleaner AAM.

These experimental results highlight that the integrating rubber into AAM materials significantly influences their physical and mechanical properties. Although the addition of rubber decreases compressive strength and flowability, it enhances the thermal and acoustic performance of the composite. Moreover, this research sheds light on the considerable impact of the MA02 curing method at 60°C on AAM properties. This approach stands out markedly by its significant enhancement of AAM compressive strength, outperforming results obtained with other methods. The economic and ecological analysis underscores the efficiency of 60°C oven curing offering a promising pathway for the production of a more environmentally friendly and economically viable material.

5. Limitations of the Current Study

While the study sheds light on the impact of rubber content on various properties of alkali-activated mortar (AAM), it has several limitations. Firstly, its findings may not be widely applicable beyond the specific experimental conditions and materials used. Additionally, the focus on short-term analysis up to 28 days limits insights into long-term performance and durability. The study's emphasis on rubber content overlooks other factors that could influence AAM properties, such as the type of activator, precursor nature, etc. Recognizing these limitations underscores the need for further research to address these gaps and provide a more holistic evaluation of AAM's performance and applicability.

6. Future Recommendations

The study highlights the effects of rubber content on alkali-activated mortar (AAM) properties, but it has limitations. It primarily focuses on short-term analysis and overlooks other factors like the type of activator and curing conditions. Future research should explore long-term performance, optimize rubber incorporation methods, conduct field trials, compare AAM with conventional materials, and expand economic and environmental assessments. These efforts will enhance understanding and optimize the

use of rubber-incorporated AAM in construction for sustainable infrastructure development.

Acknowledgement

References

[1] Luukkonen, T., et al., One-part alkali-activated materials: A review. Cement and Concrete Research, 2018. 103: p. 21-34. https://doi.org/10.1016/j.cemconres.2017.10.001

[2] Jain, A. and S. Marathe, Soft computing modeling on air-cured slag-fly ash-glass powder-based alkali activated masonry elements developed using different industrial waste aggregates. Asian Journal of Civil Engineering, 2023: p. 1-13. https://doi.org/10.1007/s42107-023-00584-7

[3] Amran, Y.M., et al., Clean production and properties of geopolymer concrete; A review. Journal of Cleaner Production, 2020. 251: p. 119679. https://doi.org/10.1016/j.jclepro.2019.119679

[4] Singh, N., M. Kumar, and S. Rai, Geopolymer cement and concrete: Properties. Materials Today: Proceedings, 2020. 29: p. 743-748. https://doi.org/10.1016/j.matpr.2020.04.513

[5] Hills, T., N. Florin, and P.S. Fennell, Decarbonising the cement sector: a bottom-up model for optimising carbon capture application in the UK. Journal of Cleaner Production, 2016. 139: p. 1351-1361. https://doi.org/10.1016/j.jclepro.2016.08.129

[6] Nakkeeran, G. and L. Krishnaraj, Developing lightweight concrete bricks by replacing fine aggregate with vermiculite: A regression analysis prediction approach. Asian Journal of Civil Engineering, 2023: p. 1-9. https://doi.org/10.1007/s42107-023-00586-5

[7] De Azevedo, A.R., et al., Use of glass polishing waste in the development of ecological ceramic roof tiles by the geopolymerization process. International Journal of Applied Ceramic Technology, 2020. 17(6): p. 2649-2658. https://doi.org/10.1111/ijac.13585

[8] Diaz-Loya, E.I., E.N. Allouche, and S. Vaidya, Mechanical properties of fly-ash-based geopolymer concrete. ACI materials journal, 2011. 108(3): p. 300.

[9] Hossain, F.Z., et al., Mechanical properties of recycled aggregate concrete containing crumb rubber and polypropylene fiber. Construction and Building Materials, 2019. 225: p. 983-996. https://doi.org/10.1016/j.conbuildmat.2019.07.245

[10] Sofi, A., Effect of waste tyre rubber on mechanical and durability properties of concrete–A review. Ain Shams Engineering Journal, 2018. 9(4): p. 2691-2700. https://doi.org/10.1016/j.asej.2017.08.007

[11] Association, U.T.M., US scrap tire management summary. US Tire Manufacturers Association: Washington, DC, USA, 2018.

[12] Long, W.-J., et al., Sustainable use of recycled crumb rubbers in eco-friendly alkali activated slag mortar: Dynamic mechanical properties. Journal of cleaner production, 2018. 204: p. 1004-1015. https://doi.org/10.1016/j.jclepro.2018.08.306

[13] Ameri, F., et al., Partial replacement of copper slag with treated crumb rubber aggregates in alkali-activated slag mortar. Construction and Building Materials, 2020. 256: p. 119468. https://doi.org/10.1016/j.conbuildmat.2020.119468

[14] Ameur Belmouhoub, Assia Abdelouahed, and Ammar Noui, Experimental and factorial design of the mechanical and physical properties of concrete containing waste rubber

Powder. Res. Eng. Struct. Mater.2023. http://dx.doi.org/10.17515/resm2023.54me0810rs

[15] Chiker, T., et al., Sodium sulfate and alternative combined sulfate/chloride action on ordinary and self-consolidating PLC-based concretes. Construction and Building Materials, 2016. 106: p. 342-348. https://doi.org/10.1016/j.conbuildmat.2015.12.123

[16] Zhao, J., et al., Workability, compressive strength, and microstructures of one-part rubberized geopolymer mortar. Journal of Building Engineering, 2023. 68: p. 106088. https://doi.org/10.1016/j.jobe.2023.106088

[17] Qaidi, S.M., et al., Rubberized geopolymer composites: A comprehensive review. Ceramics International,2022.48(17):p.24234-24259. https://doi.org/10.1016/j.ceramint.2022.06.123

[18] Park, Y., et al., Compressive strength of fly ash-based geopolymer concrete with crumb rubber partially replacing sand. Construction and Building Materials, 2016. 118: p. 43-51. https://doi.org/10.1016/j.conbuildmat.2016.05.001

[19] Athira, V., et al., Influence of different curing methods on mechanical and durability properties of alkali activated binders. Construction and Building Materials, 2021. 299: p. 123963. https://doi.org/10.1016/j.conbuildmat.2021.123963

[20] Valente, M., et al., Reducing the emission of climate-altering substances in cementitious materials: A comparison between alkali-activated materials and Portland cement-based composites incorporating recycled tire rubber. Journal of Cleaner Production, 2022. 333: p. 130013. https://doi.org/10.1016/j.jclepro.2021.130013

[21] Gill, P., et al., Effects of various additives on the crumb rubber integrated geopolymer concrete.CleanerMaterials,2023.8:p.100181. https://doi.org/10.1016/j.clema.2023.100181

[22] Zeyad, A.M., et al., Impact of rice husk ash on physico-mechanical, durability and microstructural features of rubberized lightweight geopolymer composite. Construction andBuildingMaterials,2024.427:p.136265. https://doi.org/10.1016/j.conbuildmat.2024.136265

[23] Haruna, S., et al., Effect of paste aggregate ratio and curing methods on the performance of one-part alkali-activated concrete. Construction and Building Materials, 2020. 261: p. 120024. https://doi.org/10.1016/j.conbuildmat.2020.120024

[24] Trincal, V., et al., Effect of drying temperature on the properties of alkali-activated binders-recommendations for sample preconditioning. Cement and Concrete Research, 2022. 151: p. 106617. https://doi.org/10.1016/j.cemconres.2021.106617

[25] Liu, J., et al., Study the Mechanical Properties of Geopolymer under Different Curing Conditions. Minerals, 2023. 13(5): p. 690. https://doi.org/10.3390/min13050690

[26] Luhar, S., S. Chaudhary, and U. Dave, Effect of different parameters on the compressive strength of rubberized geopolymer concrete. Multi-Disciplinary Sustainable Engineering: Current and Future Trends, 2016: p. 77-86.

[27] Rajendran, M. and M. Akasi, Performance of crumb rubber and nano fly ash based ferro-geopolymer panels under impact load. KSCE Journal of civil engineering, 2020. 24: p. 1810-1820. https://doi.org/10.1007/s12205-020-0854-z

[28] Luhar, S., S. Chaudhary, and I. Luhar, Thermal resistance of fly ash based rubberized geopolymer concrete. Journal of Building Engineering, 2018. 19: p. 420-428. https://doi.org/10.1016/j.jobe.2018.05.025

[29] Kaveh, A. and N. Khavaninzadeh. Efficient training of two ANNs using four meta-heuristic algorithms for predicting the FRP strength. in Structures. 2023. Elsevier. https://doi.org/10.1016/j.istruc.2023.03.178

[30] Narasimha Reddy, P. and J. Ahmed Naqash, Experimental study on TGA, XRD and SEM analysis of concrete with ultra-fine slag. International Journal of Engineering, 2019. 32(5): p. 679-684. https://doi.org/10.5829/ije.2019.32.05b.09

[31] Rathee, M., A. Misra, and J. Kolleboyina, Study of mechanical properties of geopolymer mortar prepared with fly ash and GGBS. Materials Today: Proceedings, 2023. 93: p. 377-386. https://doi.org/10.1016/j.matpr.2023.07.360

[32] Zhang, H.-Y., J.-C. Liu, and B. Wu, Mechanical properties and reaction mechanism of one-part geopolymer mortars. Construction and Building Materials, 2021. 273: p. 121973. https://doi.org/10.1016/j.conbuildmat.2020.121973

[33] Pham, T.M., et al., Durability characteristics of lightweight rubberized concrete. Construction and Building Materials, 2019. 224: p. 584-599. https://doi.org/10.1016/j.conbuildmat.2019.07.048

[34] advanced drying technique. Agriculture and Agricultural Science Procedia, 2014. 2: p. 26-32. https://doi.org/10.1016/j.aaspro.2014.11.005

[35] C1437, A., Standard Test Method for Flow of Hydraulic Cement Mortar. ASTM International, 1999: p. ASTM C1437-01.

[36] C642-13, A., Standard Test Method for Density, Absorption, and Voids in Hardened Concrete. ASTM International, 2013.

[37] Standard, E., Methods of testing cement-Part 1: Determination of strength. Turkish Standards Institute, Ankara, Turkey, 2009.

[38] EN.1015-18, Methods of Test for Mortar for Masonry: Determination of Water Absorption Coefficient Due to Capillary Action of Hardened Mortar 2002.

[39] Hamidi, F., A. Valizadeh, and F. Aslani. The effect of scoria, perlite and crumb rubber aggregates on the fresh and mechanical properties of geopolymer concrete. in Structures. 2022. Elsevier. https://doi.org/10.1016/j.istruc.2022.02.031

[40] Pham, T.M., Y.Y. Lim, and M. Malekzadeh, Effect of pre-treatment methods of crumb rubber on strength, permeability and acid attack resistance of rubberised geopolymer concrete. Journal of Building Engineering, 2021. 41: p. 102448. https://doi.org/10.1016/j.jobe.2021.102448

[41] Sheraz, M., et al., Fresh and hardened properties of waste rubber tires based concrete: a state art of review. SN Applied Sciences, 2023. 5(4): p. 119. https://doi.org/10.1007/s42452-023-05336-5

[42] Wongsa, A., et al., Mechanical and thermal properties of lightweight geopolymer mortar incorporating crumb rubber. Journal of Cleaner Production, 2018. 195: p. 1069-1080. https://doi.org/10.1016/j.jclepro.2018.06.003

[43] Abd-Elaty, M.A.A., M.F. Ghazy, and O.H. Khalifa, Mechanical and Impact Properties of Fibrous Rubberized Geopolymer Concrete. Mansoura Engineering Journal, 2023. 48(4): p. 5. https://doi.org/10.58491/2735-4202.3054

[44] Zhai, S., et al., Effect of modified rubber powder on the mechanical properties of cement-based materials. Journal of Materials Research and Technology, 2022. 19: p. 4141-4153. https://doi.org/10.1016/j.jmrt.2022.06.070

[45] Nematollahi, B., J. Sanjayan, and F.U.A. Shaikh, Synthesis of heat and ambient cured one-part geopolymer mixes with different grades of sodium silicate. Ceramics International, 2015. 41(4): p. 5696-5704. https://doi.org/10.1016/j.ceramint.2014.12.154

[46] Lương, Q.-H., et al., Effects of crumb rubber particles on mechanical properties and sustainability of ultra-high-ductile slag-based composites. Construction and Building Materials, 2021. 272: p. 121959. https://doi.org/10.1016/j.conbuildmat.2020.121959

[47] Ali, I.M., A.S. Naje, and M.S. Nasr, Eco-friendly chopped tire rubber as reinforcements in fly ash based geopolymer concrete. Glob. Nest J., 2020. 22: p. 342-7. https://doi.org/10.30955/gnj.003192

[48] Kirgiz, M.S., Advancements in mechanical and physical properties for marble powder–cement composites strengthened by nanostructured graphite particles. Mechanics of Materials, 2016. 92: p. 223-234. https://doi.org/10.1016/j.mechmat.2015.09.013

[49] Dean, A. and D. Voss, Design and analysis of experiments. 1999: Springer. https://doi.org/10.1007/0-387-22634-6_15

[50] Lawson, J., Design and Analysis of Experiments with R. Vol. 115. 2014: CRC press.

[51] Kaveh, A., Applications of metaheuristic optimization algorithms in civil engineering. 2017: Springer.

[52] Khanzadi, M., et al., Optimization of building components with sustainability aspects in BIM environment: Optimization of building components with sustainability aspects in BIM environment. Periodica Polytechnica Civil Engineering, 2019. 63(1): p. 93-103. https://doi.org/10.3311/PPci.12551

[53] Goupy, J. and L. Creighton, Introduction to design of experiments with JMP examples. 2007: SAS publishing. https://doi.org/10.1145/3289402.3289534

[54] Xie, J., et al., Effects of the addition of silica fume and rubber particles on the compressive behaviour of recycled aggregate concrete with steel fibres. Journal of Cleaner Production, 2018. 197: p. 656-667. https://doi.org/10.1016/j.jclepro.2018.06.237

[55] Yahya, Z., et al. Durability of fly ash based geopolymer concrete infilled with rubber crumb in seawater exposure. in IOP Conference Series: Materials Science and Engineering. 2018. IOP Publishing. https://doi.org/ 10.1088/1757-899X/374/1/012069

[56] Al Bakria, A.M., et al., The effect of curing temperature on physical and chemical properties of geopolymers. Physics Procedia, 2011. 22: p. 286-291. https://doi.org/10.1016/j.phpro.2011.11.045

[57] Mathew, G. and B. Joseph, Flexural behaviour of geopolymer concrete beams exposed to elevated temperatures. Journal of Building Engineering, 2018. 15: p. 311-317. https://doi.org/10.1016/j.jobe.2017.09.009

[58] Dehdezi, P.K., S. Erdem, and M.A. Blankson, Physico-mechanical, microstructural and dynamic properties of newly developed artificial fly ash based lightweight aggregate–Rubber concrete composite. Composites Part B: Engineering, 2015. 79: p. 451-455. https://doi.org/10.1016/j.compositesb.2015.05.005

[59] Ma, C., et al., Preparation of cleaner one-part geopolymer by investigating different types of commercial sodium metasilicate in China. Journal of Cleaner Production, 2018. 201: p. 636-647. https://doi.org/10.1016/j.jclepro.2018.08.060

[60] Samarakoon, M., et al., Properties of one-part fly ash/slag-based binders activated by thermally-treated waste glass/NaOH blends: A comparative study. Cement and Concrete Composites, 2020. 112: p. 103679. https://doi.org/10.1016/j.cemconcomp.2020.103679

[61] Ma, C., et al., Properties and characterization of green one-part geopolymer activated by composite activators. Journal of Cleaner Production, 2019. 220: p. 188-199. https://doi.org/10.1016/j.jclepro.2019.02.159

[62] Chiaia, B., et al., Eco-mechanical index for structural concrete. Construction and Building Materials, 2014. 67: p. 386-392. https://doi.org/10.1016/j.conbuildmat.2013.12.090

[63] Maddalena, R., J.J. Roberts, and A. Hamilton, Can Portland cement be replaced by low-carbon alternative materials? A study on the thermal properties and carbon emissions of innovative cements. Journal of Cleaner Production, 2018. 186: p. 933-942. https://doi.org/10.1016/j.jclepro.2018.02.138

[64] Perez-Cortes, P. and J.I. Escalante-Garcia, Alkali activated metakaolin with high limestone contents–Statistical modeling of strength and environmental and cost analyses. Cement and Concrete Composites, 2020. 106: p. 103450. https://doi.org/10.1016/j.cemconcomp.2019.103450

[65] Jiang, M., et al., Comparative life cycle assessment of conventional, glass powder, and alkali-activated slag concrete and mortar. Journal of Infrastructure Systems, 2014. 20(4): p. 04014020. https://doi.org/10.1061/(ASCE)IS.1943-555X.0000211